IOPscience iopscience.iop.org

Home Search Collections Journals About Contact us My IOPscience

Annealing in GaInNAs system

This article has been downloaded from IOPscience. Please scroll down to see the full text article.

2004 J. Phys.: Condens. Matter 16 S3229

(http://iopscience.iop.org/0953-8984/16/31/017)

View the table of contents for this issue, or go to the journal homepage for more

Download details:
IP Address: 129.252.86.83
The article was downloaded on 27/05/2010 at 16:22

Please note that terms and conditions apply.

INSTITUTE OF PHYSICS PUBLISHING JOURNAL OF PHYSICS: CONDENSED MATTER

J. Phys.: Condens. Matter **16** (2004) S3229–S3244 PII: S0953-8984(04)75292-3

Annealing in GaInNAs system

Masahiko Kondow[1], **Takeshi Kitatani**[1] **and Sho Shirakata**[2]

[1] Central Research Laboratory, Hitachi Ltd, 1-280 Higashi-Koigakubo, Kokubunji, Tokyo 185-8601, Japan
[2] Faculty of Engineering, Ehime University, 3 Bunkyou-cho, Matsuyama, Ehime 790-8577, Japan

E-mail: kondow@crl.hitachi.co.jp

Received 20 January 2004
Published 23 July 2004
Online at stacks.iop.org/JPhysCM/16/S3229
doi:10.1088/0953-8984/16/31/017

Abstract

The effect of post-growth thermal annealing on crystallinity and bandgap in GaInNAs systems is systematically investigated. Annealing greatly improves the crystallinity of GaInNAs and also blue shifts the bandgap. This improved crystallinity is due to the elimination of non-radiative centres, and is not directly related to the blue shift in the bandgap. The blue shift may be closely related to the red shift in the bandgap seen when N is added to GaInNAs; if so, this would provide a clue to the reasons for the red shift in the bandgap of III–N–V alloys. The unexpected behaviour of the bandgap in GaInNAs is investigated by examining the bonds through optical phonons. We have found that the bandgap varies with the strength or length of the GaN bonds in GaInNAs. Annealing changes atomic positions in a unit cell of GaInNAs and thus blue shifts its bandgap.

1. Introduction

GaInNAs is a novel optoelectronic material that was proposed and created by the authors [1]. It is regarded as a breakthrough material in terms of realizing long-wavelength vertical-cavity surface-emitting laser diodes, which are urgently required as light sources for next-generation local area networks [2]. GaInNAs is suitable for this application because it is a narrow-gap semiconductor that can be pseudomorphically grown on a GaAs substrate. Alloying Ga(In)As with N decreases both the lattice constant and the bandgap [1]. The red shift in the bandgap caused by alloying with wide-gap nitrides is unexpected but is interesting in terms of both basic science and semiconductor technology. The reason for the red shift has been studied from both theoretical [3–7] and experimental [8–10] perspectives. According to first-principles calculations by Rubio and Cohen [4], a *volume effect* is the main reason. The GaN bonds are extended when they are in the Ga(In)As lattice. Electrons localized around the N atoms, which are far from the Ga atoms, pull down the bottom energy level of the conduction band. As a result, the bandgap shrinks. Shan *et al* [8] have experimentally shown that an energy band of

© 2004 IOP Publishing Ltd Printed in the UK

N is generated above the bottom of the Ga(In)As host crystal's conduction band, and that the bandgap is reduced by repulsion between the N band and the conduction band. Jones *et al* [10] reported that the repulsion is due to band-mixing of the X point or L point with the Γ point, rather than the energy band of N. In any case, the main effect of alloying with N is on the conduction band, the bottom of which is lowered, and has little effect on the valence band.

The small N atom means that III–N–V alloys such as GaInNAs and GaNAs are thermodynamically metastable or unstable. It is generally difficult to obtain excellent crystallinity for crystals of these materials. Post-growth thermal annealing is effective as a way of improving the optical properties of III–N–V alloys [11]. In GaInNAs, annealing greatly increases the photoluminescence (PL) intensity and concurrently blue shifts the PL peak wavelength. In a $Ga_{1-x}In_xN_yAs_{1-y}$ ($x = 0.3$, $y = 0.01$)/GaAs quantum well, which is used as the active layer of 1.3 μm-range laser diodes, the red shift due to alloying with N, and the subsequent blue shift due to annealing, are typically 150 and 50 meV, respectively [12]. Thus, the blue shift cancels out one-third of the red shift. Therefore, this issue is industrially significant for the use of GaInNAs as a narrow-gap material. A possible reason for the blue shift is intermixing of In and/or N atoms at hetero-interfaces between GaInNAs and GaAs. However, experiments have shown that the bandgap of a thick GaInNAs layer is also blue shifted by annealing [12]. Therefore, the blue shift in peak PL wavelength is mainly attributable to the bandgap shift. The reason for the blue shift in bandgap may be closely related to the reason for the red shift in bandgap for III–N–V alloys and thus provide a key to the reasons for this red shift.

A bandgap shift of over 50 meV is extraordinary for a III–V semiconductor with a fixed composition. In $Ga_{0.5}In_{0.5}P$, which is used in red-light-emitting laser diodes, a CuPt-type long-range ordered structure is spontaneously formed under certain conditions of growth. The bandgap is narrower by approximately 50 meV than that of the randomly arranged alloy [13]. Therefore, we may expect that a similar variation in the atomic structure of GaInNAs occurs during the annealing. Since the material's N content is small, at only a few per cent, long-range ordered structures might not form or may be highly imperfect. Indeed, no ordered structures have yet been found in transmission electron microscopy (TEM) observations. Klar *et al* [14] attributed the blue-shifted bandgap to short-range ordering. They explained that a rearrangement of the N nearest-neighbour environments from Ga-rich to In-rich (from $N–Ga_4$ to $In–N–Ga_3$, $In_2–N–Ga_2$, $In_3–N–Ga$ or $In_4–N$) changes the bandgap. However, Harmand *et al* [15] also observed a blue-shifted bandgap also in GaNAsSb, which of course does not contain indium atoms, and in which N is always bonded with four Ga atoms. Thus, there must be another reason for the blue-shifted bandgap. According to first-principles calculations by Bellaiche *et al* [6, 7], the band structure of the III–N–V alloys is sensitive to *atomic relaxation*, i.e. variation in atomic positions within unit cells, as well as the *volume effect*. Hence, if annealing changes the degree of atomic relaxation in III–N–V alloys, the bandgap should also vary. Might atomic relaxation of III–N–V alloys be the main reason for the blue shift in bandgap caused by annealing?

To the best of our knowledge, however, there is no concrete information on the atomic relaxation of III–N–V alloys. Even those calculations in which atomic relaxation is taken into account are not in good agreement with experimental results on, for example, band lineup [16] and the alloy composition dependence of the bandgap in the N-rich region [17]. This lack of agreement may be because the atomic relaxation model for conventional III–V alloys was used in the calculations. Since the discrepancy between atomic radii in III–N–V alloys is several times greater than that in conventional III–V alloys, the atomic relaxation of III–N–V alloys is probably different from that of conventional alloys. Thus, atomic relaxation in III–N–V alloys and the effect of annealing on this have remained completely unexplained. One way of

experimentally investigating atomic relaxation in III–N–V alloys is to use optical phonons to examine the bonds in these alloys.

In this paper, we systematically investigate the effects of post-growth thermal annealing on crystallinity and bandgap in the GaInNAs system. The reason for the blue shift in the bandgap may be closely related to the reason for the red shift in the bandgap of GaInNAs and thus provide us with a key to understanding the reason for the red shift in the bandgap of III–N–V alloys. The unexpected behaviour of the bandgap in GaInNAs was investigated by using optical phonons to examine the bonds. The results are discussed. The blue shift seen in the bandgap is explicable in terms of a general concept of atomic relaxation.

The subject matter of this paper is organized as follows. In section 2, the effect of annealing on the crystallinity and bandgap of GaInNAs is examined. Annealing was found to improve crystallinity by eliminating non-radiative centres, and is not directly related to the blue shift in the bandgap. We also report on the results of our use of optical phonons to investigate the atomic bonds in terms of the blue shift in the bandgap. This material is in section 3. In section 4, we describe the effect of annealing on bonds in GaInNAs. This is followed by a discussion of the reason for the unexpected behaviour of the bandgap in GaInNAs. Finally, we conclude the paper in section 5.

2. The effects of annealing on the crystallinity and bandgap of GaInNAs

In this section, we discuss our use of two structures to examine the effect of annealing on the crystallinity and bandgap of GaInNAs. One structure was a $Ga_{0.3}In_{0.7}N_{0.01}As_{0.99}$ single quantum well (GaInNAs-SQW), in which a 7 nm-thick GaInNAs layer was sandwiched between GaAs barrier layers; the other was a 1 μm-thick $Ga_{0.95}In_{0.05}N_{0.02}As_{0.98}$ bulk layer (bulk GaInNAs) lattice-matched with GaAs. A $Ga_{0.3}In_{0.7}As$ SQW (GaInAs-SQW) with the same structure as the GaInNAs-SQW was also employed for reference. All were grown by molecular beam epitaxy (MBE). Details of the sample preparation are given elsewhere [12]. *In situ* annealing was done in the MBE chamber after crystal growth for 1 h, at temperatures of 500, 550, 600 or 650 °C, under an As_2 beam.

The dependence of the room-temperature PL characteristics on temperature of annealing is shown in figure 1. For the GaInNAs-SQW, the shift in wavelength versus the change in annealing temperature was 0.23 meV $°C^{-1}$, i.e. more than three times the corresponding value for the GaInAs-SQW, which was 0.06 meV $°C^{-1}$ (figure 1(a)). PL from the GaInAs-SQW was intense and was almost constant across the range of annealing temperatures. The PL peak intensity of the GaInNAs-SQW, on the other hand, showed a marked increased with thermal annealing, approaching the same level as that for the GaInAs-SQW when annealing was at 550 °C (figure 1(b)). The optimal annealing temperature varies with the as-grown crystallinity of the GaInNAs. Results for both PL peak wavelength and peak PL intensity for bulk GaInNAs were similar to those for the GaInNAs-SQW.

The square of the absorption coefficient α multiplied by the square of the photon energy (E) is shown in figure 2 as a function of the photon energy of other samples of bulk GaInNAs. These samples had a layered structure that was almost the same as that of bulk GaInNAs sample mentioned above, and were annealed at 500, 600, or 650 °C. The absorption-band edges are clearly blue shifted by annealing, and the degree of this blue shift increases with temperature of annealing. The bandgap was estimated from a point determined by linear extrapolation of the spectra; specifically from the point where the dotted lines in figure 2 cross the x-axis. The bandgap energy is thus blue shifted even in the bulk GaInNAs. The rate of increase in bandgap with temperature of annealing was 0.26 meV $°C^{-1}$, which is very close to the value for the increase in PL energy with temperature of annealing for bulk GaInNAs: 0.24 meV $°C^{-1}$.

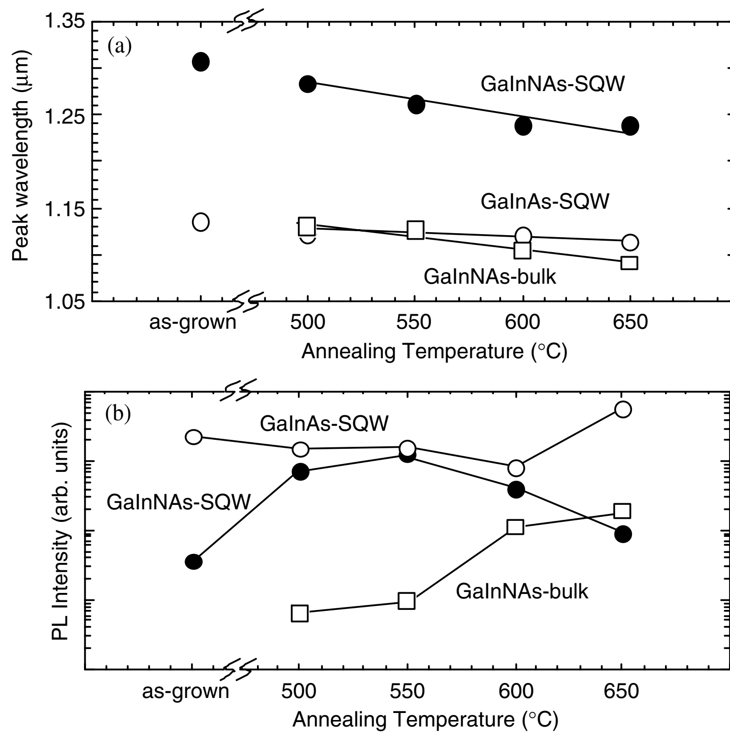

Figure 1. Dependence of PL characteristics on *in situ* annealing temperature: (a) peak wavelength and (b) intensity [12].

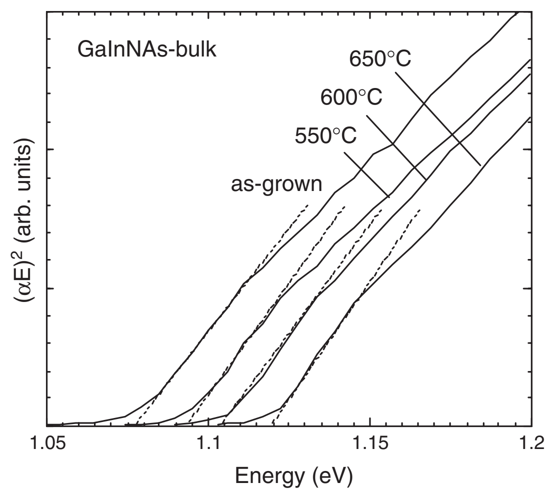

Figure 2. Absorption spectra of bulk GaInNAs layers annealed at various temperatures [12].

Thus, a large bandgap shift in the GaInNAs well should lead to a large shift in PL energy from the QW structure. Secondary ion mass spectrometry (SIMS) and x-ray diffraction showed that annealing did not affect the proportions of either In or N. This indicates that the blue shift in the bandgap is not due to a compositional change.

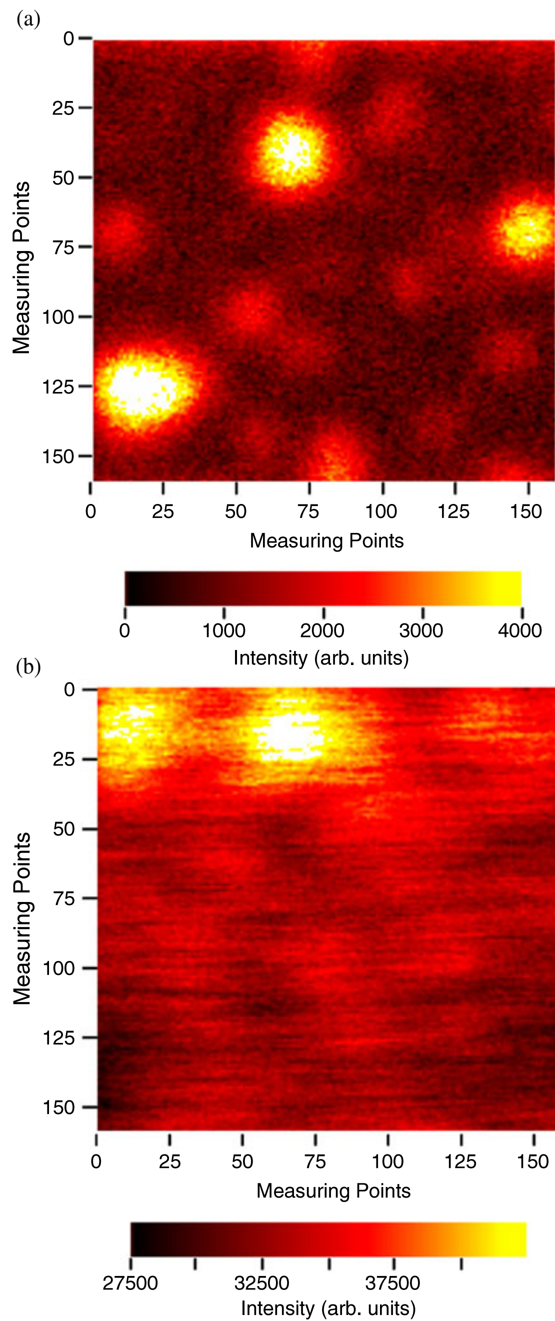

Figure 3. Comparison of the CL mappings for a GaInNAs-SQW at 30 K: (a) as-grown and (b) after 600 °C *in situ* annealing [12].

(This figure is in colour only in the electronic version)

Cathodoluminescence (CL) mappings of the GaInNAs-SQW at 30 K are given in figure 3. The CL wavelengths before and after annealing at 600 °C were set to the main peak wavelengths

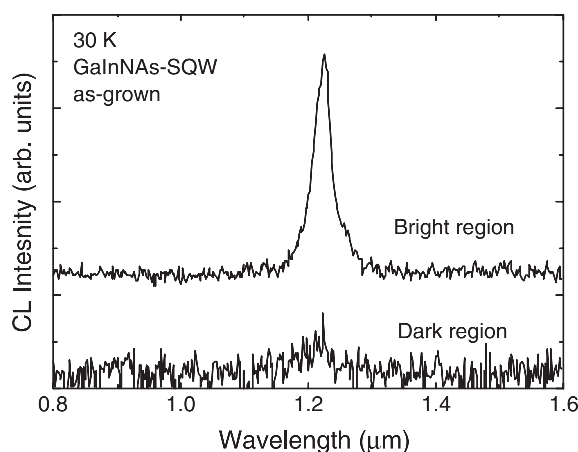

Figure 4. CL spectra for the bright and dark regions of the CL map of the as-grown GaInNAs SQW [12].

at 1.222 and 1.148 μm, respectively. The emission image from the as-grown sample is non-uniform and dot-like. The CL-intensity range in the mapping was from zero to 4000, so the CL is 1000 times as intense in the bright regions as in the dark regions. After thermal annealing at 600 °C, the CL intensity of the sample increased to the range from 27 500 to 42 500. In this case, CL is less than twice as intense in the bright regions as in the dark regions. (Note that very different intensity ranges are used in (a) and (b) of figure 3.) Thermal annealing clearly leads to a dramatic improvement in uniformity of the CL intensity across the whole mapping image.

CL spectra from both the bright and dark regions of the CL map for an as-grown GaInNAs-SQW are shown in figure 4. In the bright region, a peak at 1.222 μm is clearly visible. The peak CL intensity in the dark region is much lower. Both regions have almost the same peak wavelength. Thus, the dark region was not formed by wavelength fluctuation due to variation in either the In or N content or to variation in the thickness of the GaInNAs well. The main reason for the higher PL intensity seen after thermal annealing must be an improvement in the intensity of emission over the entire region. This greater uniformity is probably a result of the elimination of non-radiative centres (preventing the formation of non-radiative centres in the as-grown GaInNAs layer requires careful optimization of both growth and post-annealing). The improvement is not directly related to the blue shift in the bandgap of GaInNAs, because the bandgaps of the bright and dark regions in the as-grown crystal are blue shifted by the same amount.

3. Optical phonon energies in GaInNAs

Atomic relaxation can be investigated by using optical phonon energies to examine the bonds. To determine the phonon energies in GaInNAs, the authors systematically studied optical phonons in GaInAs, GaNAs and GaInNAs by using both Raman scattering (RS) and infrared (IR) absorption spectroscopy. Since In- and N-related phonons in GaInNAs are very weak due to the small proportions of In and N, detecting them is quite difficult. We thus found it useful to compare the results with data on the constituent materials, i.e. GaInAs and GaNAs.

Samples were grown on a 350 μm-thick (100) semi-insulating GaAs wafer. The indium content x and nitrogen content y in $Ga_{1-x}In_xN_yAs_{1-y}$ were $7\pm2\%$ and $2\pm0.5\%$, respectively. Thus, the GaInNAs layer was nearly lattice-matched with the GaAs substrate. GaNAs and

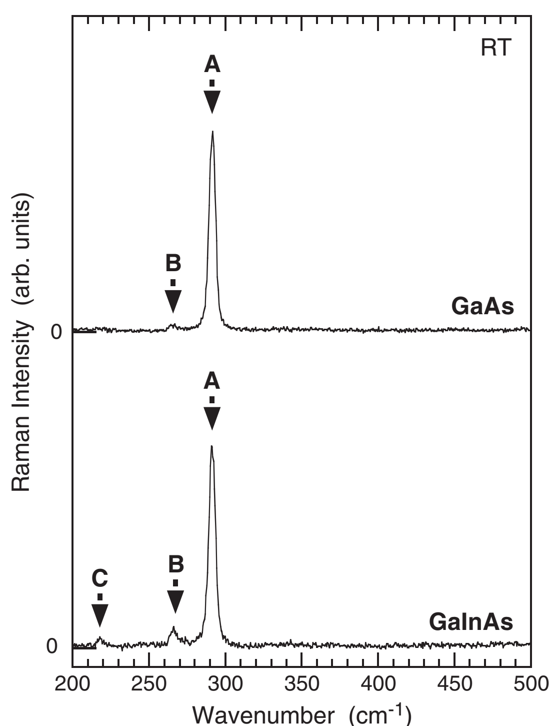

Figure 5. RS spectra of GaAs and $Ga_{0.93}In_{0.07}As$. Labels A, B and C denote the GaAs-LO, GaAs-TO and InAs-LO phonons, respectively.

GaInAs with the same proportion of either N or In as the GaInNAs were also grown. The lattice mismatch in both GaNAs and GaInAs was approximately 0.5%. The $Ga_{0.93}In_{0.07}N_{0.02}As_{0.98}$ layers were 0.5 or 1.0 μm thick. On the other hand, the thicknesses of the $GaN_{0.02}As_{0.98}$ and $Ga_{0.93}In_{0.07}As$ layers were reduced to 0.1 μm to avoid misfit dislocations. The samples in this section were as-grown (not annealed).

Raman scattering spectra were measured in the back-scattering configuration. The excitation light was the 514.5 nm line of an Ar ion laser. The scattered light was detected by using a double-monochromator and photon counter. With the scattering geometry used in this study, longitudinal optical (LO) phonons were primarily measured according to the Raman selection rule for the zinc-blende lattice.

Figure 5 shows the RS spectra of $Ga_{0.93}In_{0.07}As$ and the reference GaAs wafer measured at room temperature (RT). In the GaAs spectrum, the LO phonon peak (A) and the TO phonon peak (B) appear at 292 and 268 cm^{-1}, respectively. The full width at half maximum (FWHM) for the LO phonon peak was 5 cm^{-1}. The forbidden TO mode appears as a consequence of angular deviations in the optical path, the sample placement, crystallographic misorientation of the wafer, and perhaps other factors.

In the spectrum for GaInAs, the LO and TO phonons of the GaAs bonds appeared at 291 cm^{-1} and around 268 cm^{-1}, respectively. Although the GaInAs layer was thinner (at 0.1 μm) than the depth of penetration ($\approx$0.3 μm) of the 514.5 nm line of the Ar laser, the measured spectrum was mainly due to the GaInAs layer, judging from the fact that the LO-phonon energy of the GaAs bonds was shifted from 292 to 291 cm^{-1}. This red shift by 1 cm^{-1} was a consequence of alloying with In. The FWHM of the LO-phonon peak for the GaAs bonds was unchanged at 5 cm^{-1}. On the other hand, the intensity of the forbidden TO

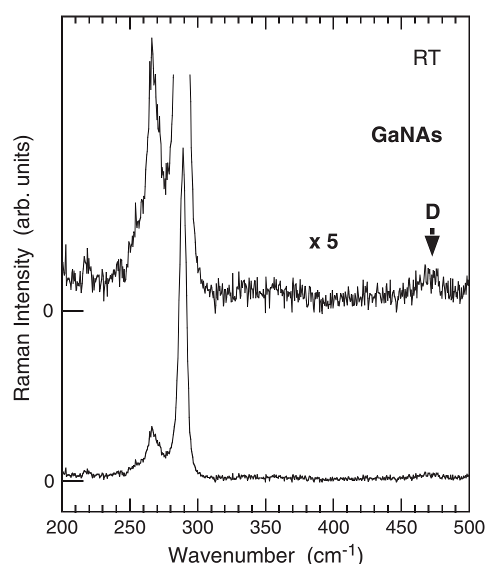

Figure 6. RS spectrum of $GaN_{0.02}As_{0.98}$. Label D denotes the GaN-LO phonon.

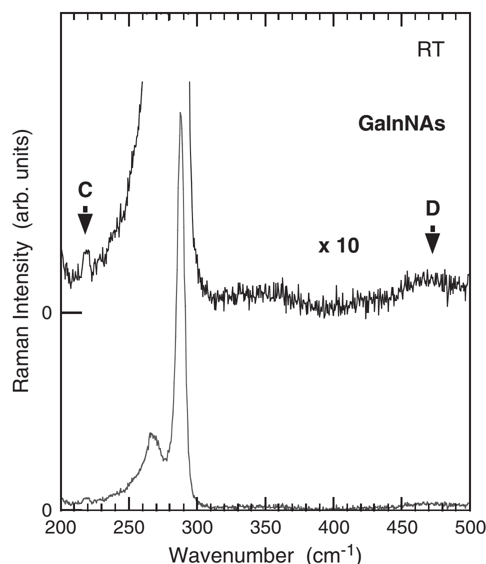

Figure 7. RS spectrum of $Ga_{0.93}In_{0.07}N_{0.02}As_{0.98}$. Labels C and D denote the InAs-LO and GaN-LO phonons, respectively.

mode of the GaAs bonds was greater than that for GaAs. This intensity increase is due to the relaxation of the Raman selection rule because of *disorder* in the alloy. This disorder has two components. One is the random placement of Ga and In atoms at column III lattice sites. The other is deformation of the lattice itself, i.e. *atomic relaxation*. Thus, the TO-mode intensity is affected by atomic relaxation. A further small peak (C) appeared at around 218 cm^{-1}. Soni *et al* [18] reported that the LO-phonon energy of InAs bonds in $Ga_{0.47}In_{0.53}As$ was 230 cm^{-1}. In general, alloying weakens bonds so that they produce phonons with less energy [19]. Since our sample of $Ga_{0.93}In_{0.07}As$ had a lower proportion of In than the sample used by Soni *et al*, the LO-phonon energy of the InAs bonds was expected to be below 230 cm^{-1}. Thus, peak C was attributed to the LO phonons of the InAs bonds. The InAs bonds have low phonon intensity for two reasons. Firstly, the proportion of In was low, at approximately 7%. Secondly, phonon intensity is low for In-related bonds in general [19, 20].

Figure 6 shows the RS spectrum of GaNAs at two scales (1× and 5× magnified); this is similar to a result reported by Mintairov *et al* [21]. Peaks corresponding to the LO and TO phonons of the GaAs bonds appeared at 289 cm^{-1} and around 268 cm^{-1}, respectively. A peak that corresponds to the LO phonon of the GaN bonds [21] appears at around 473 cm^{-1} (D). The low Raman intensity of the GaN bonds was probably a consequence of the low N content, which was only approximately 2%. The energy of the GaAs-LO phonon in GaNAs was red-shifted by 3 cm^{-1} in comparison with that in GaAs. Its FWHM increased to 6 cm^{-1}. The GaAs TO mode in GaNAs was more intense than that for GaInAs.

Figure 7 shows the RS spectrum of GaInNAs at 10× magnification. This is similar to the spectrum for GaNAs (figure 6). While the individual peaks are broader, adding In to GaNAs did not significantly affect the overall spectrum. This spectrum is also similar to one reported by Hashimoto *et al* [22]. Peaks corresponding to the LO and TO phonons of the GaAs bonds appeared at 288 cm^{-1} and around 268 cm^{-1}, respectively. A peak that corresponds to the LO phonon of the GaN bonds appeared at around 473 cm^{-1}. The peak for GaN-LO phonons

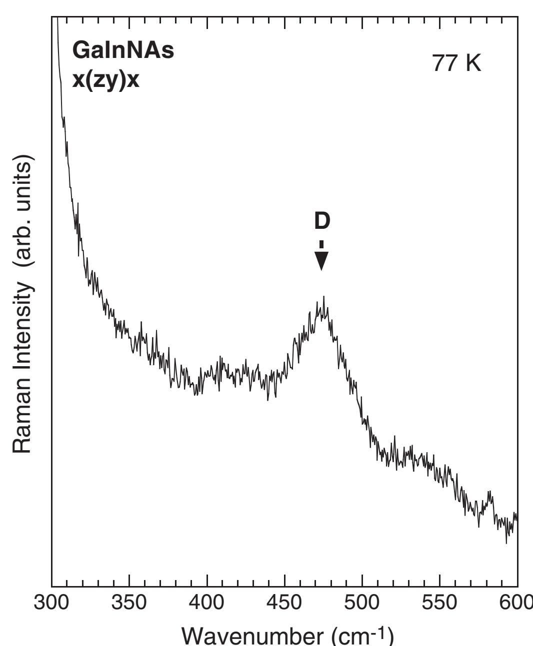

Figure 8. RS spectrum of $Ga_{0.93}In_{0.07}N_{0.02}As_{0.98}$ as measured in the $x(zy)x$ configuration at 77 K. Label D denotes the GaN-LO phonon.

was weaker and broader than that from GaNAs. The energy of the GaAs-LO phonon was red shifted by a further 1 cm^{-1} from the energy level for GaNAs, and its FWHM was also higher (7 cm^{-1}). The peak corresponding to the GaAs-TO mode was stronger and broader than that for GaNAs. While a small peak corresponding to the InAs-LO phonon appeared at around 218 cm^{-1}, it was less intense than the corresponding peak in GaInAs.

To reduce the background level due to double-frequency signals from phonons with low energy levels with the aim of more clearly observing the peak of the GaN-LO phonon in GaInNAs, we measured polarization [23]. Figure 8 shows the RS spectrum of GaInNAs measured in the $x(zy)x$ configuration at 77 K. A distinct peak again appears at around 473 cm^{-1} (D). However, no Raman signal due to the InN bonds in GaInNAs was detected. Considering the ratio between the intensity of the phonons from the InAs and GaAs bonds shown in figure 5 and the GaN phonon intensity shown in figure 8, we see that detecting phonons from InN bonds through RS measurement is quite difficult.

Infrared absorption measurements are sensitive to the phonons from N-related bonds because the transmitted light contains much information about the epilayers. For IR measurements, the transmission of infrared light transmitted through the sample was analysed by using a Fourier transform infrared (FT-IR) measurement system. The IR spectrum of the epilayer was obtained by subtracting the spectrum for a reference GaAs wafer from the raw spectrum. The GaAs substrate was strongly absorbent at wavelengths below 350 cm^{-1}. Therefore, the IR measurements were more suitable for examining the bonds of the nitrides than those of the arsenides. Under the conditions of measurement, transverse optical (TO) phonons were primarily measured according to the selection rule unlike the case for Raman scattering measurements.

Figure 9 shows the IR spectra for GaNAs and GaInNAs as measured at RT. In both spectra, a strong peak (E) appears at around 470 cm^{-1}. This peak energy is close to the LO-phonon

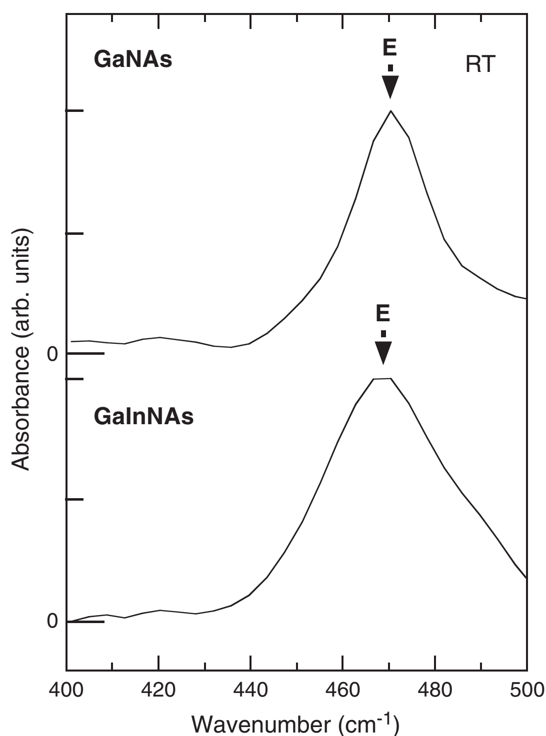

Figure 9. IR spectra of $GaN_{0.02}As_{0.98}$ and $Ga_{0.93}In_{0.07}N_{0.02}As_{0.98}$ measured at RT. Label E denotes the GaN-TO phonon.

energy of the GaN bonds shown in figures 6–8. In general, when the alloy composition is very low, the energy discrepancy between the TO and LO modes is negligible, and the two modes converge on the impurity-local-vibration mode. Riede *et al* [24] has studied the IR absorption spectra of GaAs with N impurities (but not the GaNAs alloy) and reported that the local vibration mode of the N impurities was 470 cm^{-1}. The peaks labelled E are in good agreement with this result. Therefore, the peaks at 470 cm^{-1} in GaNAs and GaInNAs are attributable to the TO phonons from the GaN bonds. Note that the GaN-TO phonon peak was broader for GaInNAs than for GaNAs.

Next, we attempted to determine the phonon energy of the InN bonds in GaInNAs. Experimental noise was suppressed by performing IR-absorption measurements at a very low temperature [25]. Figure 10 shows the spectrum for GaInNAs measured at 8 K. The strong peak (E) that corresponds to the TO mode of the GaN bonds is again seen at 470 cm^{-1}. The peak had the same energy even at room temperature (the difference between the peak energy at 8 K and at RT might be within the limiting resolution of energy in this measurement of 4 cm^{-1}). A small but distinct peak labelled F appears at 407 cm^{-1}. It must have also been present in the result obtained at room temperature (figure 9), but was not visible because it was at the same intensity as the noise level.

The three results below indicate that the peak at 407 cm^{-1} is attributable to the TO mode which corresponds to the InN bond in GaInNAs [25].

(1) The peak was only seen in the spectrum for GaInNAs, i.e. it was not visible in the spectrum for GaNAs.

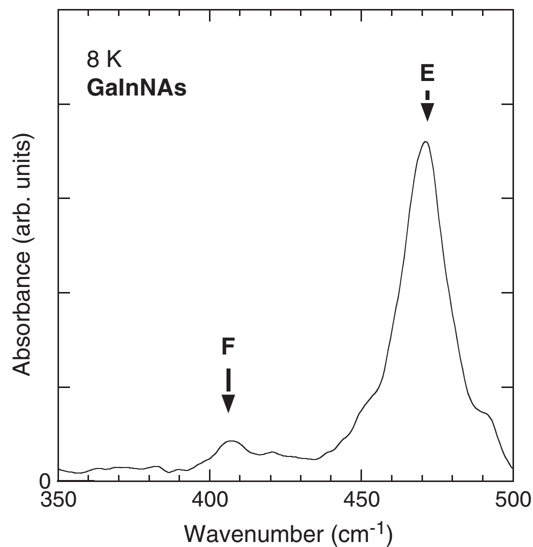

Figure 10. IR spectrum of $Ga_{0.93}In_{0.07}N_{0.02}As_{0.98}$ measured at 8 K (layer thickness: 1.0 μm). Labels E and F denote the GaN-TO and InN-TO phonons, respectively.

Table 1. Variation in Raman signals for GaAs bonds in GaInAs, GaNAs, and GaInNAs alloys relative to the signals for GaAs.

Material	Red shift of LO phonons (cm^{-1})	Broadening of LO phonons (cm^{-1})	Intensity ratio of TO to LO phonons (%)
GaAs	N/A	N/A	2.5
GaInAs	1	0	8.6
GaNAs	3	1	15.0
GaInNAs	4	2	19.5

(2) The ratio of the intensity of the peak at 407 to that at 470 cm^{-1} agrees with the proportion of indium to gallium in the sample crystal and thus reflects the ratio between the numbers of indium–nitrogen and gallium–nitrogen bonds.

(3) As was shown above, the TO-phonon energy for the GaN bond in GaInNAs is 470 cm^{-1}. This is red shifted by 85 cm^{-1} from the result for a pure binary lattice of GaN (555 cm^{-1}) [26], indicating that the GaN bond is weakened or elongated in the GaInNAs lattice. The InN bond must be affected in the same way within the GaInNAs lattice. Since the lattice mismatch between the individual binary crystals and the GaInNAs drives the elongation or weakening of the nitrogen-related bonds, the red shift in the phonon energy of the nitrogen-related bonds may be assumed to be proportional to the lattice mismatch between the individual binary crystals and GaInNAs. Figure 11 clearly shows the proportionality between the red shift of the phonon energy and the lattice mismatch. By analogy with GaN bonds, the InN bonds may produce an LO-phonon peak at around 410 cm^{-1}.

Table 1 summarizes the differences between Raman signals for the GaAs bonds in GaInAs, GaNAs and GaInNAs alloys from those for GaAs. As the degree of atomic relaxation is increased by alloying, the LO-phonon energy is red shifted, the LO-phonon peak becomes broader, and the intensity ratio of the TO to LO phonons increases. Since N has a much smaller

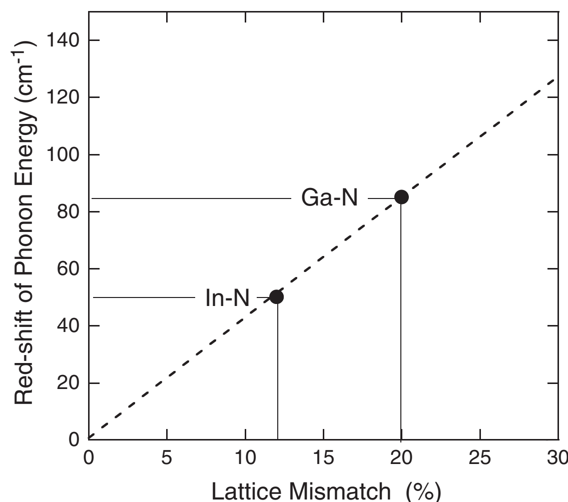

Figure 11. Red shift of TO-phonon energies for the GaN and InN bonds in GaInNAs from the values for the respective binary crystals (GaN or InN) versus the lattice mismatch between the individual binary crystals (GaN or InN) and GaInNAs [25]. In this plot, the phonon energy for the indium–nitrogen bond in a pure InN binary lattice is 457 cm^{-1} [26], while the corresponding value for GaInNAs is assumed to be 407 cm^{-1}. The lattice constant of the GaInNAs samples used in this study is equal to that of GaAs. The broken line in the figure is a guide for the eye.

atomic radius than Ga, In or As, alloying with N clearly leads to greater atomic relaxation than alloying with In, even though the lattice mismatches in GaNAs and GaInAs are almost the same. The atomic relaxation in GaInNAs is greater than that in GaNAs.

4. The effect of annealing on atomic relaxation in GaNAs and GaInNAs

In this section, we investigate the effect of annealing on atomic relaxation in GaInNAs. The bonds in GaInNAs were examined by IR-absorption spectroscopy. The bandgap and crystallinity of GaInNAs were studied by photoreflectance (PR). The samples used in this section are basically the same as used in section 3. The measurements were done both before and after thermal annealing.

For the PR measurements, the pumping light was the 514.5 nm line from an Ar-ion laser, while the probe light was white light from a W–halogen lamp. The reflected probe light was analysed by using a monochromator and then phase-sensitively detected by a cooled GaInAs p–i–n photodiode. These measurements were performed at RT.

Figure 12 shows PR spectra around the bandgap before and after rapid thermal annealing (RTA) at 700 °C for 30 s. During the RTA, the samples were placed on a GaAs wafer in a face-to-face configuration, since this prevented the out-diffusion of As. The GaInNAs layer was 500 nm thick. Since the samples were almost strain-free, the spectra were simple and were thus analysed by using third-derivative functional forms (unlike those reported by Klar *et al* [14], the PR spectra measured by the authors were simple, and this was true even of those measured at 80 K; no fine structure due to the change in the N nearest-neighbour environments was visible). The bandgaps denoted by the arrows in figure 12 were blue shifted by 58 meV after annealing. This shift is in good agreement with that in the absorption spectra for GaInNAs (figure 2). Note that RTA increased the PR intensity approximately 10-fold and decreased the broadening factor from 32 to 11 meV. These results indicate a dramatic improvement in

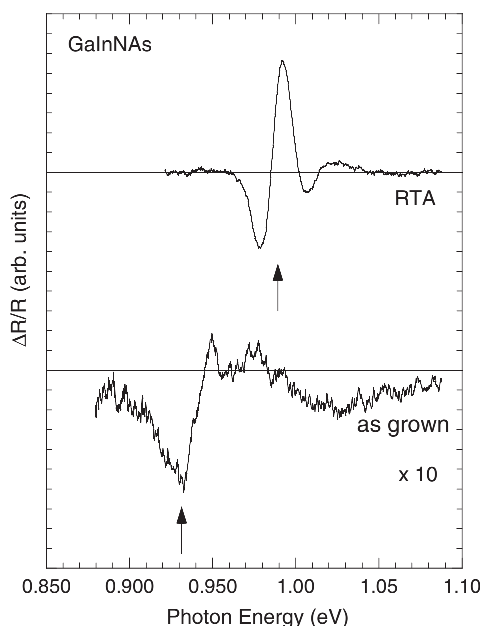

Figure 12. PR spectra for as-grown and annealed GaInNAs measured at RT. Arrows indicate the bandgaps.

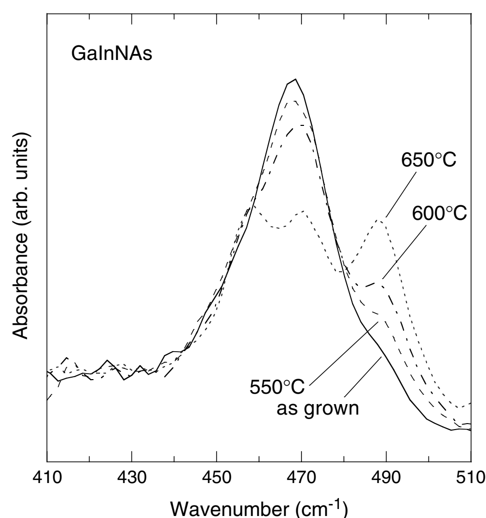

Figure 13. IR spectra for as-grown and annealed GaInNAs measured at RT.

the crystallinity of GaInNAs from the viewpoint of PR. In PL measurements, RTA increased the intensity approximately 100-fold so that it reached the same level as that for GaInAs, a conventional III–V semiconductor.

Figure 13 shows results for the dependence of the IR spectra for GaInNAs on temperature of annealing [27]. The samples were annealed *in situ* in the MBE chamber under an As_2 beam. The temperature of annealing was precisely varied from 550 to 650 °C, and annealing was applied for 1 h. The intensity of the peak at 470 cm^{-1} decreased as the temperature increased. At high temperatures of annealing, additional peaks appeared at 460 and 490 cm^{-1} (Kurtz *et al* [28] have reported similar results). This demonstrates that GaN bonds exhibit three vibration modes in GaInNAs. This phenomenon, in which a single type of bond in an alloy semiconductor exhibits multiple vibration modes that correspond to different levels of phonon energy, has not previously been reported, and is a special property of GaInNAs. By using Gaussian forms to decompose each spectrum into the three peaks at 460, 470 and 490 cm^{-1}, we found that the total intensity did not change, and that the intensity of the peak at 460 cm^{-1} was almost independent of the annealing temperature. Thus, as the peak intensity at 470 cm^{-1} decreased, the peak intensity at 490 cm^{-1} increased. This means that the transition from the peak at 470 cm^{-1} to that at 490 cm^{-1} with rising temperature of annealing, probably originates in alternation to the GaN-bond state. The authors examined GaInNAs samples with slight compressive strain and slight tensile strain, but the results were unchanged. Therefore, the results given in figures 12 and 13 are independent of this kind of strain.

A bond is formed between by two atoms, while the a bandgap is formed by a number of atoms *en masse*. Even if there are different kinds of bonds in an alloy, the alloy has a single bandgap as long as the phase is uniform. For example, in a conventional alloy of InGaAsP,

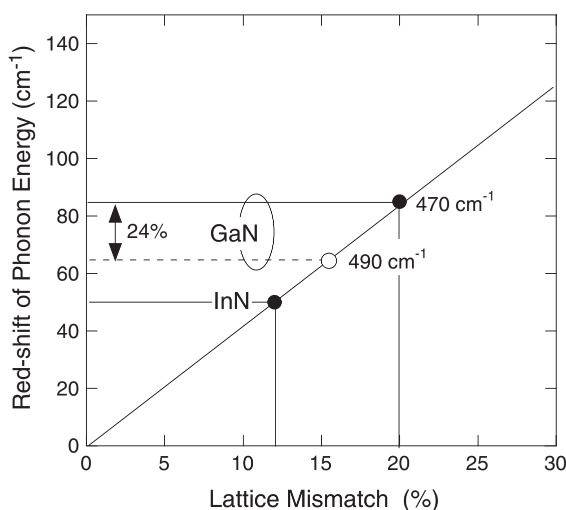

Figure 14. Red-shift of TO phonon energies of the GaN and InN bonds in GaInNAs from those in the respective binary crystals, versus the lattice mismatch between GaInNAs and the respective binary crystals. Filled circles are for as-grown materials; the open circle is for the annealed material.

there are four kinds of bond, i.e. Ga–P, In–P, Ga–As and In–As. However, the alloy has a single bandgap. Thus, it is possible for GaInNAs to have a single bandgap as shown in figure 12, even if though the Ga–N bond has three kinds of states.

In general, the phonon-energy levels in III–V semiconductors are not particularly sensitive to external conditions such as temperature and pressure. The phonon-energy shift of 20 cm^{-1} seen in figure 13 is anomalous for a III–V semiconductor. This may be due to an internal change in the GaInNAs crystal, i.e. to atomic relaxation. Since the IR-absorption peaks for larger-bandgap semiconductors with smaller bond lengths are generally seen in the region of higher energy, the blue-shifted phonon energy of the GaN bonds indicates shortening of the bonds. The main reason for the red shift in the bandgap of GaInNAs is a *volume effect* i.e. extension of the GaN bonds [4], so shortening of the GaN bonds probably accounts for the annealing-induced blue shift of the bandgap.

Next, the authors attempted to quantitatively evaluate the annealing-induced change in the GaN bond length within GaInNAs. Figure 11 reveals that the red shift in the phonon energy of nitrogen-related bonds is proportional to the lattice mismatch between the individual binary crystals and the GaInNAs. Hence, the red shift in the phonon energy of the nitrogen-related bonds can be used as a tentative measure of bond extension in GaInNAs. On this basis, the authors estimated that the GaN bonds corresponding to a TO phonon energy of 490 cm^{-1} are shorter by 24% than those for GaN bonds corresponding to a TO-phonon energy of 470 cm^{-1}, as is shown in figure 14.

When the temperature of annealing is 650 °C, the degree of absorption was roughly the same at 470 and 490 cm^{-1} (figure 13). This indicates that roughly equal numbers of GaN bonds are in the states corresponding to the respective wavenumbers. The GaN bonds corresponding to 490 cm^{-1} were 24% shorter than those corresponding to 470 cm^{-1}. The bandgap of this *in situ* annealed sample was 1.12 eV, which represents a blue shift of 45 meV from the result for the as-grown sample. These results could be keys to an understanding of atomic relaxation in GaInNAs. In the future, calculations that are consistent with these experimental results should reveal details of the structure of atomic relaxation in III–N–V alloys.

Next, we discuss the mechanism responsible for the annealing-induced change in bond length or atomic relaxation in GaInNAs. Non-radiative centres are present in as-grown GaInNAs, and are eliminated during annealing (the results in figure 3 demonstrate this effect). TEM observations by the authors (data are not shown) indicated that GaInNAs is free of stacking defaults and misfit dislocations. The non-radiative centres are probably point defects, such as vacancies. Van Vechten proposed a model in which the movements of vacancies lead to alternation of the arrangement of atoms in the lattice [29]. Therefore, the migration of point defects may produce a rearrangement of the sites of atoms. During this atomic rearrangement, the elongated GaN bond might make a transition to a lower energy state corresponding to a shorter bond and, thus, the atomic relaxation might be generated. The background carrier density in our as-grown GaInNAs was low, in the 10^{15} cm^{-3} range, and conductivity was n-type. Even though some compensation occurs with p-type defects, this indicates the presence of far fewer point defects than GaN bonds. However, the above atomic rearrangement is plausible, since all atoms in the paths of moving point defects would be rearranged. When the point defects are made to wander about and are then extinguished by the annealing, the atomic relaxation may be the means for a transition to a state with lower internal energy.

5. Conclusions

The effect of post-growth thermal annealing on crystallinity and bandgap in GaInNAs has been systematically investigated. Annealing greatly improved the crystallinity of GaInNAs, concurrently blue shifting the bandgap. The improved crystallinity is due to the elimination of non-radiative centres, so this effect is not directly related to the blue shift in the bandgap of GaInNAs. The blue shift in bandgap may be closely related to the red shift in bandgap of III–N–V alloys and thus provide us with a key to a better understanding of the reasons for the red shift in the bandgap of III–N–V alloys. To investigate the unexpected bandgap behaviour of GaInNAs, we observed optical phonons as a way of examining the bonds between the constituent atoms. The bandgap was found to vary with the strength or length of the GaN bonds. This result confirmed that a *volume effect* is the main reason for the red shift in the bandgap of III–N–V alloys and that the bandgap is sensitive to *atomic relaxation*. In the future, calculations that are based on these and subsequent experimental results will reveal the detailed structure of the atomic relaxation in GaInNAs.

Acknowledgment

This work was partly supported by the Japanese Government's TAO (Telecommunications Advancement Organization).

References

[1] Kondow M, Uomi K, Niwa A, Kitatani T, Watahiki S and Yazawa Y 1996 *Japan. J. Appl. Phys.* **35** 1273
[2] Ebeling K J 2000 *Proc. 13th IEEE/LEOS Annual Mtg (Rio Grande, Puerto Rico)* p PLE3
[3] Sakai S, Ueta Y and Terauchi Y 1993 *Japan. J. Appl. Phys.* **32** 4413
[4] Rubio A and Cohen M 1995 *Phys. Rev.* B **51** 4343
[5] Neugebauer J and Van de Walle C G 1995 *Phys. Rev.* B **51** 10568
[6] Bellaiche L, Wei S H and Zunger A 1996 *Phys. Rev.* B **54** 17568
[7] Bellaiche L, Wei S H and Zunger A 1997 *Appl. Phys. Lett.* **70** 3558
[8] Shan W, Walukiewicz W, Ager J W III, Haller E E, Geisz J F, Friedman D J, Olson J M and Kurtz S R 1999 *Phys. Rev. Lett.* **82** 1221

[9] Perkins J D, Mascarenhas A, Zhang Y, Geisz J F, Friedman D J, Olson J M and Kurtz S R 1999 *Phys. Rev. Lett.* **82** 3312
[10] Jones E D, Modine N A, Allerman A A, Kurtz S R, Wright A F, Tozer S T and Wei X 1999 *Phys. Rev.* B **60** 4430
[11] For example Rao E V K, Ougazzaden A, Le Bellogo Y and Juhel M 1998 *Appl. Phys. Lett.* **72** 1409
[12] Kitatani T, Nakahara K, Kondow M, Uomi K and Tanaka T 2000 *J. Cryst. Growth* **209** 345
[13] For example Kondow M, Kakibayashi H and Minagawa S 1988 *J. Cryst. Growth* **88** 291
[14] Klar P J, Grüning H, Koch J, Schäfer S, Volz K, Stolz W and Heimbrodt W 2001 *Phys. Rev.* B **64** 121203
[15] Harmand J C, Li L, Travers L, Largeau L, Patriarche G and Jusserand B 2002 *Int. Research Workshop on Physics and Technology of Dilute Nitrides for Optical Communications (Istanbul, Turkey)* p M0-5
[16] Kitatani T, Kondow M, Kikawa T, Yazawa Y, Okai M and Uomi K 1999 *Japan. J. Appl. Phys.* **38** 5003
[17] Iwata K, Asahi H, Asami K, Kuroiwa R and Gonda S 1998 *Japan. J. Appl. Phys.* **37** 1436
[18] Soni R K, Abbi S C, Jain K P, Balkanski M, Slempkes S and Benchimol J L 1986 *J. Appl. Phys.* **59** 2184
[19] Brodsky M H and Lucovsky G 1968 *Phys. Rev. Lett.* **21** 990
[20] Kondow M, Minagawa S and Satoh S 1987 *Appl. Phys. Lett.* **51** 2001
[21] Mintairov A M, Blagnov P A, Melehin V G, Faleev N N, Merz J L, Qiu Y, Nikishin S A and Temkin H 1997 *Phys. Rev.* B **56** 15836
[22] Hashimoto A, Furuhata T, Kitano T, Nguyen A K, Masuda A and Yamamoto A 2001 *J. Cryst. Growth* **227/228** 532
[23] Shirakata S 2003 *64th Autumn Mtg of the Japan Society of Applied Physics (Fukuoka, Japan)* p 1p-K-14 (Abstracts) (in Japanese)
[24] Riede V, Neuman H, Sobotta H, Schwabe R, Seifert W and Shwetlick S 1986 *Phys. Status Solidi* a **93** K151
[25] Kondow M, Kitatani T and Shirakata S 2003 *Japan. J. Appl. Phys.* **42** 4286
[26] Tabata A, Lima A P, Teles L K, Scolfaro L M, Leite J R, Lemos V, Scottker B, Frey T, Schikora D and Lischka K 1999 *Appl. Phys. Lett.* **74** 362
[27] Kitatani T, Kondow M and Kudo M 2001 *Japan. J. Appl. Phys.* **40** L750
[28] Kurtz S, Webb J, Gedvilas L, Friedman D, Geisz J, Olson J, King R, Joslin D and Karam N 2001 *Appl. Phys. Lett.* **78** 748
[29] Van Vechten J A 1982 *J. Appl. Phys.* **53** 7082